Supplementary Information

Water use efficiency responses in contrasting agroecosystems and land management practices in West Africa

Souleymane Sy[1*], Jan Bliefernicht[1], Kiril Manevski[2], Samuel Guug[3], Luitpold Hingerl[1,4], Benjamin Quesada[5], Francis E. Oussou[6], Ralf Kiese[4], Patrick Davies[7], Thomas Jagdhuber[8], Patrick Laux[4], Moussa Waongo[9], Amadou Coulibaly[9], Frank Neidl[4], Rainer Steinbrecher[4], Emmanuel Quansah[7], Seyni Salack[3], Leonard K. Amekudzi[7] and Harald Kunstmann[1,4,10*]

[1]University of Augsburg, Institute of Geography, Chair for Regional Climate and Hydrology, Augsburg, Germany

[2]Department of Agroecology, Aarhus University, Centre for Circular Bioeconomy, Tjele, Denmark

[3]West African Science Service Centre on Climate Change and Adapted Land Use, WASCAL Competence Centre, Ouagadougou, Burkina Faso

[4]Institute of Meteorology and Climate Research IMK-IFU Karlsruhe Institute of Technology, Germany

[5]Universidad del Rosario, Faculty of Natural Sciences, "Interactions Climate-Environment (ICE)" Research Group, Earth System Sciences Program, Bogotá, Colombia

[6]Federal University of Technology, Akure (FUTA), Nigeria

[7]Kwame Nkrumah University of Science and Technology, Kumasi, Ghana,

[8]Deutsches Zentrum für Luft- und Raumfahrt (DLR), German-Aerospace-Center, Germany

[9]AGRHYMET Regional Centre, Niamey, Niger

[10]University of Augsburg, Center for Climate Resilience, Augsburg, Germany

*Corresponding authors: souleymane.sy@uni-a.de, harald.kunstman@kit.edu

Submitted to: npj Sustainable Agriculture

Research type: Article

Figure S1: Energy balance closure over the study period across ecosystem types. The degree of energy balance closure is shown for each ecosystem type throughout the study period, illustrating the consistency of measured energy fluxes across contrasting land cover types.

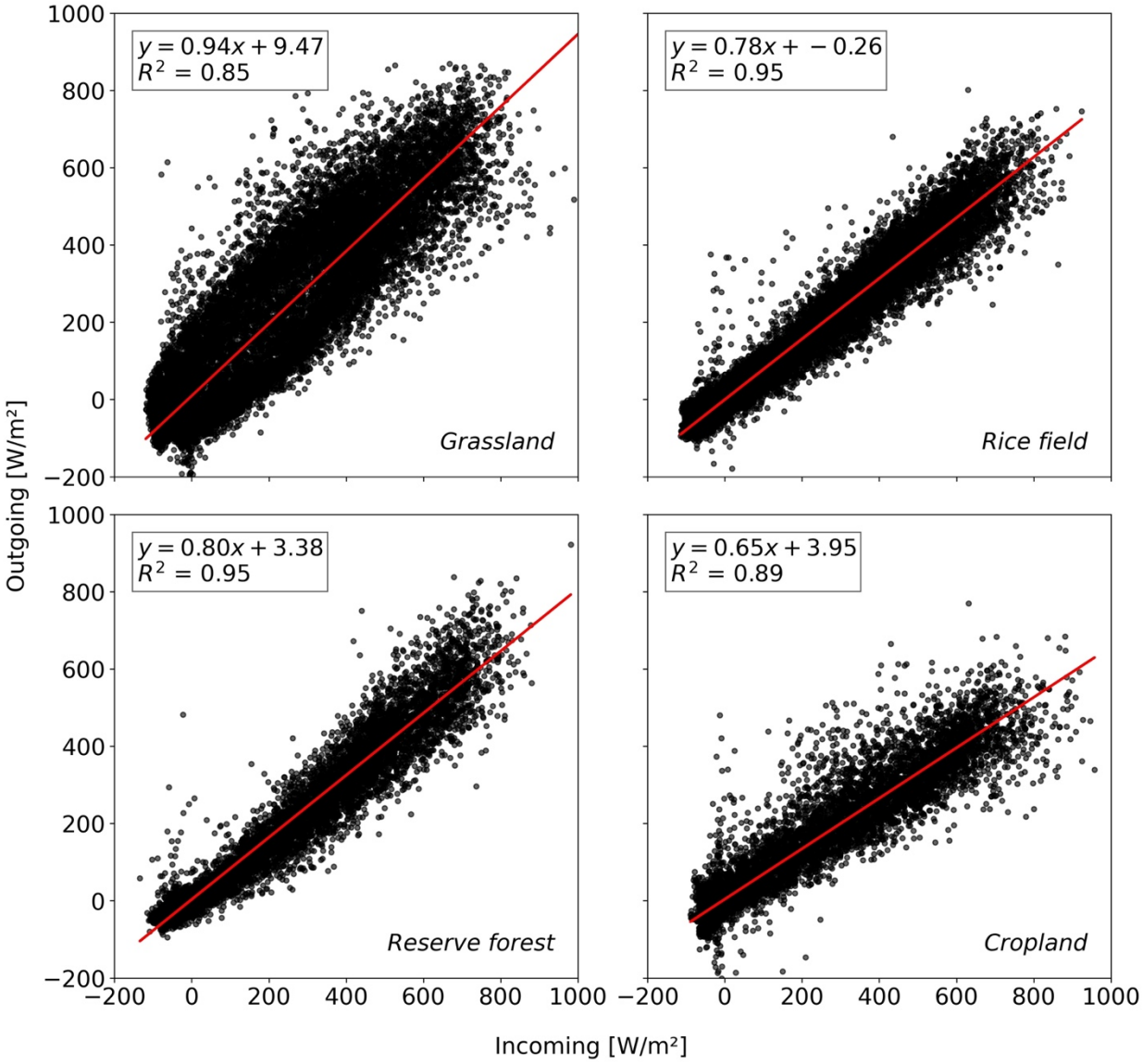

Figure S2: Diurnal GPP and ET across dry (red) and wet (blue) seasons (30-min data); error bars represent ±95% CI.

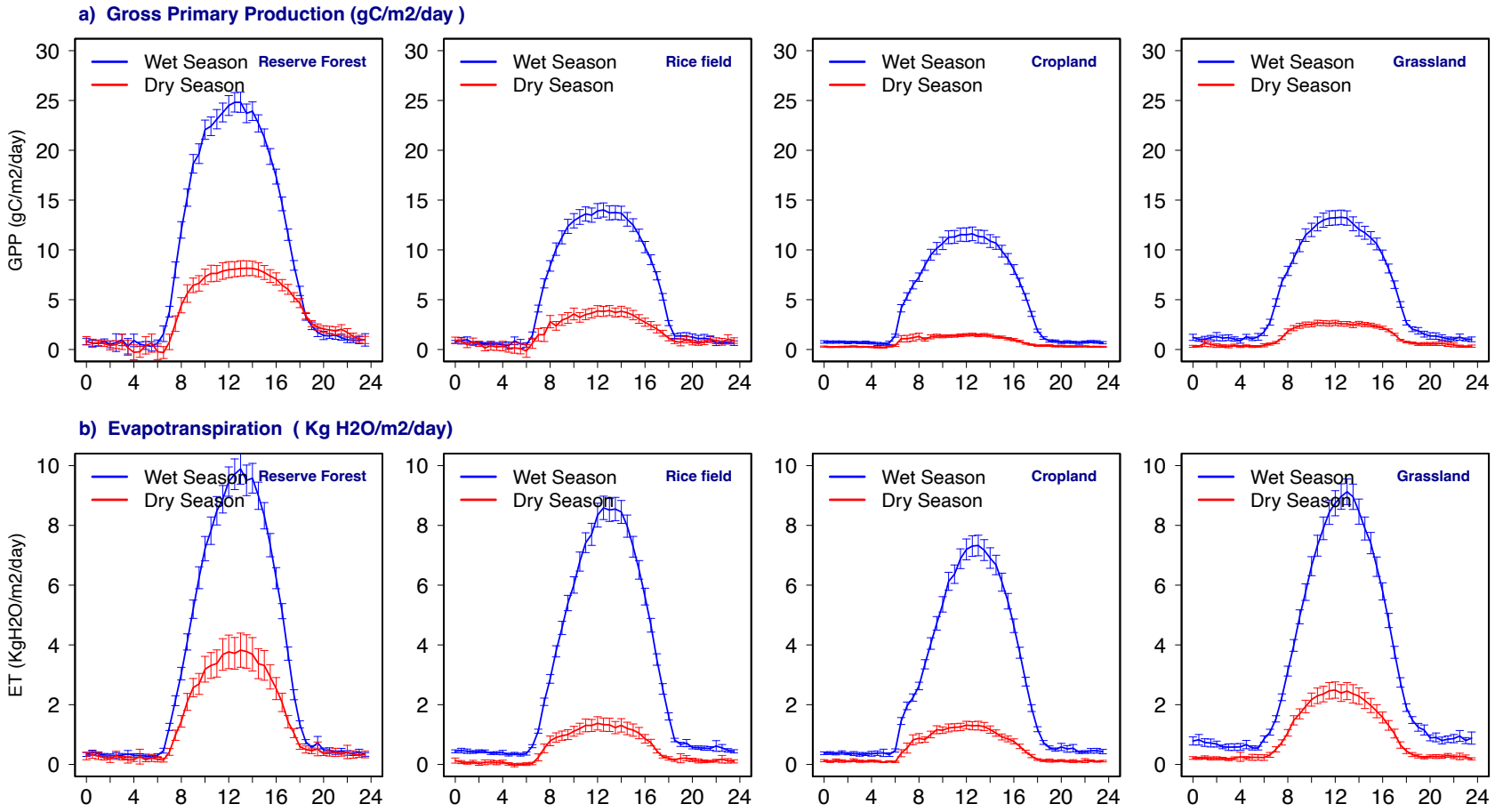

Figure S3: Diurnal VPD and Rg across dry (red) and wet (blue) seasons (30-min data); error bars represent ±95% CI.

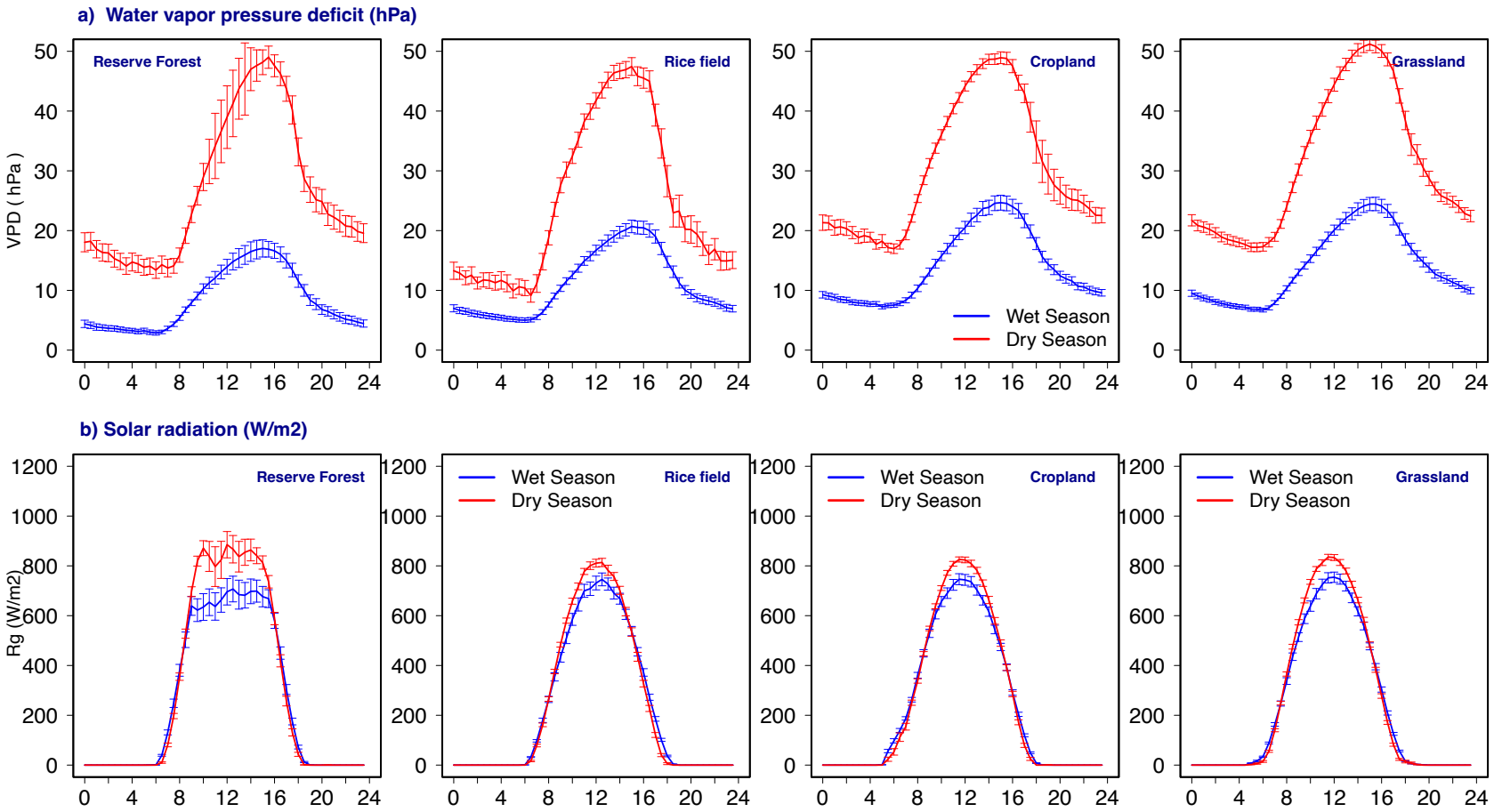

Figure S4: Diurnal Ta and RH across dry (red) and wet (blue) seasons (30-min data); error bars represent ±95% CI.

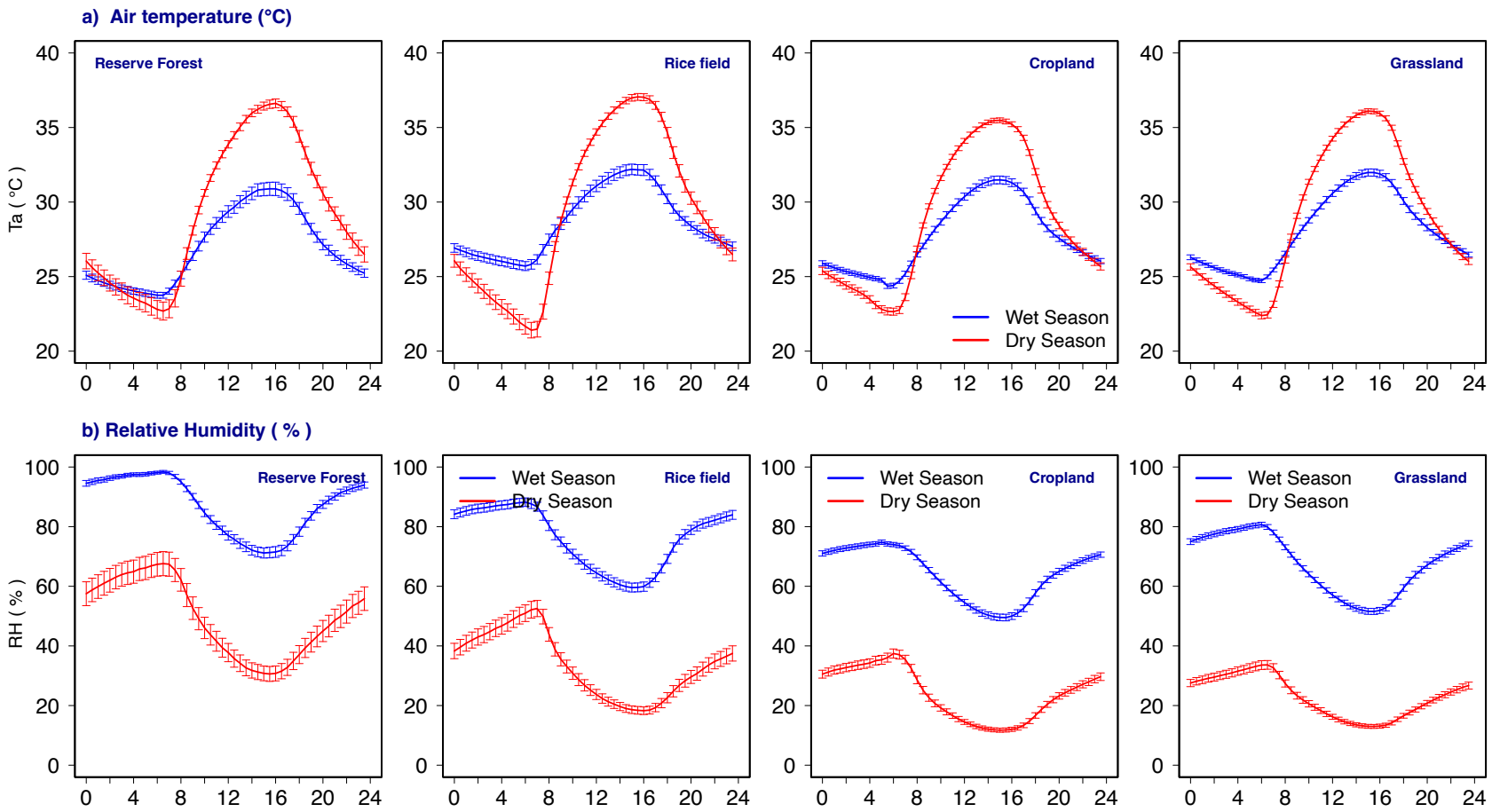

Figure S5: Annual variation in Leaf Area Index (LAI) and precipitation across all study sites. The leaf area index (LAI, m^2/m^2) was obtained from the Copernicus Land Monitoring Service (CLMS) dataset, which provides global 300 m LAI data every 10 days since 2014 (Fuster et al., 2020). The blue bars represent the monthly cumulative rainfall across all study sites. Grey shading indicates the wet season (May to October).

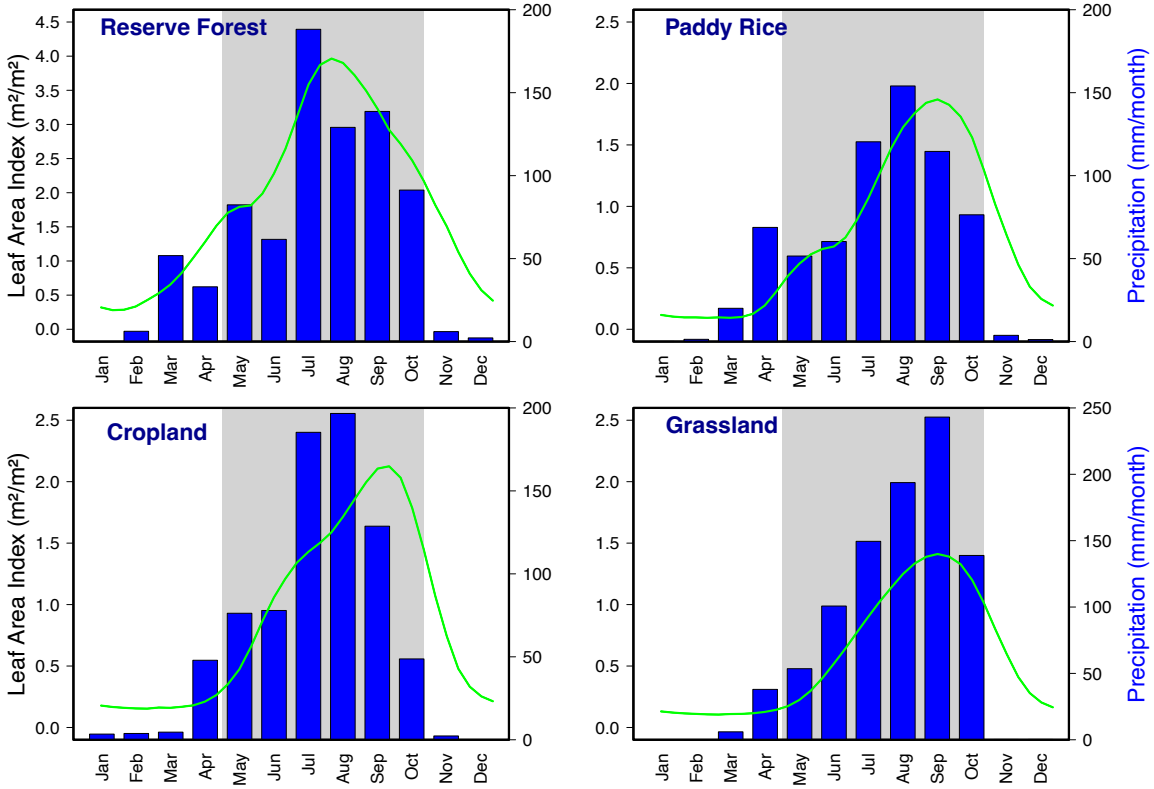

Figure S6: Environmental drivers of variance in underlying **water-use efficiency (uWUE) across ecosystem types.** The relative proportion of variance in WUE explained by each environmental variable is shown for all ecosystem types. Variables include air temperature (T_a), relative humidity (RH), vapour pressure deficit (VPD), soil moisture at 3 cm and 30 cm depths (SWC3 and SWC30), and solar radiation (Rg). Green bars denote significant contributions ($p < 0.05$; 95% confidence interval), while red bars indicate non-significant contributions ($p > 0.05$; 95% confidence interval). Grey bars represent the residual term, with the low residual values indicating that the model effectively captures the dominant environmental controls on WUE.

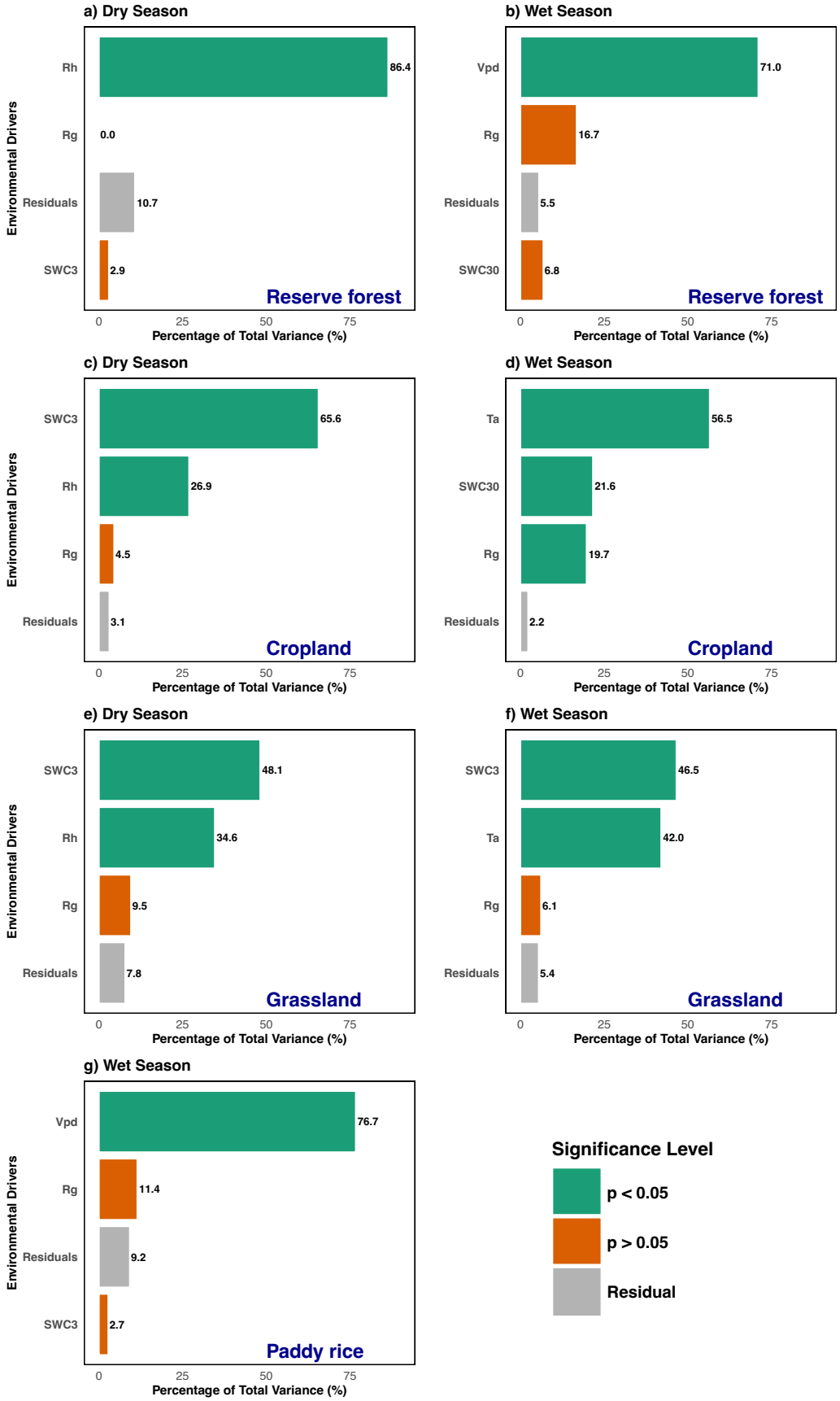
a) Dry Season
Rh
Rg
Residuals
SWC3
86.4
0.0
10.7
2.9
Reserve forest
Environmental Drivers
0
25
50
75
Percentage of Total Variance (%)
b) Wet Season
Vpd
Rg
Residuals
SWC30
71.0
16.7
5.5
6.8
Reserve forest
0
25
50
75
Percentage of Total Variance (%)
c) Dry Season
SWC3
Rh
Rg
Residuals
65.6
26.9
4.5
3.1
Cropland
Environmental Drivers
0
25
50
75
Percentage of Total Variance (%)
d) Wet Season
Ta
SWC30
Rg
Residuals
56.5
21.6
19.7
2.2
Cropland
0
25
50
75
Percentage of Total Variance (%)
e) Dry Season
SWC3
Rh
Rg
Residuals
48.1
34.6
9.5
7.8
Grassland
Environmental Drivers
0
25
50
75
Percentage of Total Variance (%)
f) Wet Season
SWC3
Ta
Rg
Residuals
46.5
42.0
6.1
5.4
Grassland
0
25
50
75
Percentage of Total Variance (%)
g) Wet Season
Vpd
Rg
Residuals
SWC3
76.7
11.4
9.2
2.7
Paddy rice
Environmental Drivers
0
25
50
75
Percentage of Total Variance (%)
Significance Level
p < 0.05
p > 0.05
Residual

Figure S7: Eddy covariance flux footprints for the different ecosystem sites: (a) reserve forest, (b) cropland, (c) paddy rice field, and (d) grassland. Footprints were calculated for each site using the method of Kljun et al. (2015). The black cross is the flux tower for each site. The outermost upwind red contour lines indicate the distance (m) within which 50% and 90% of the measured flux contribution is generated.

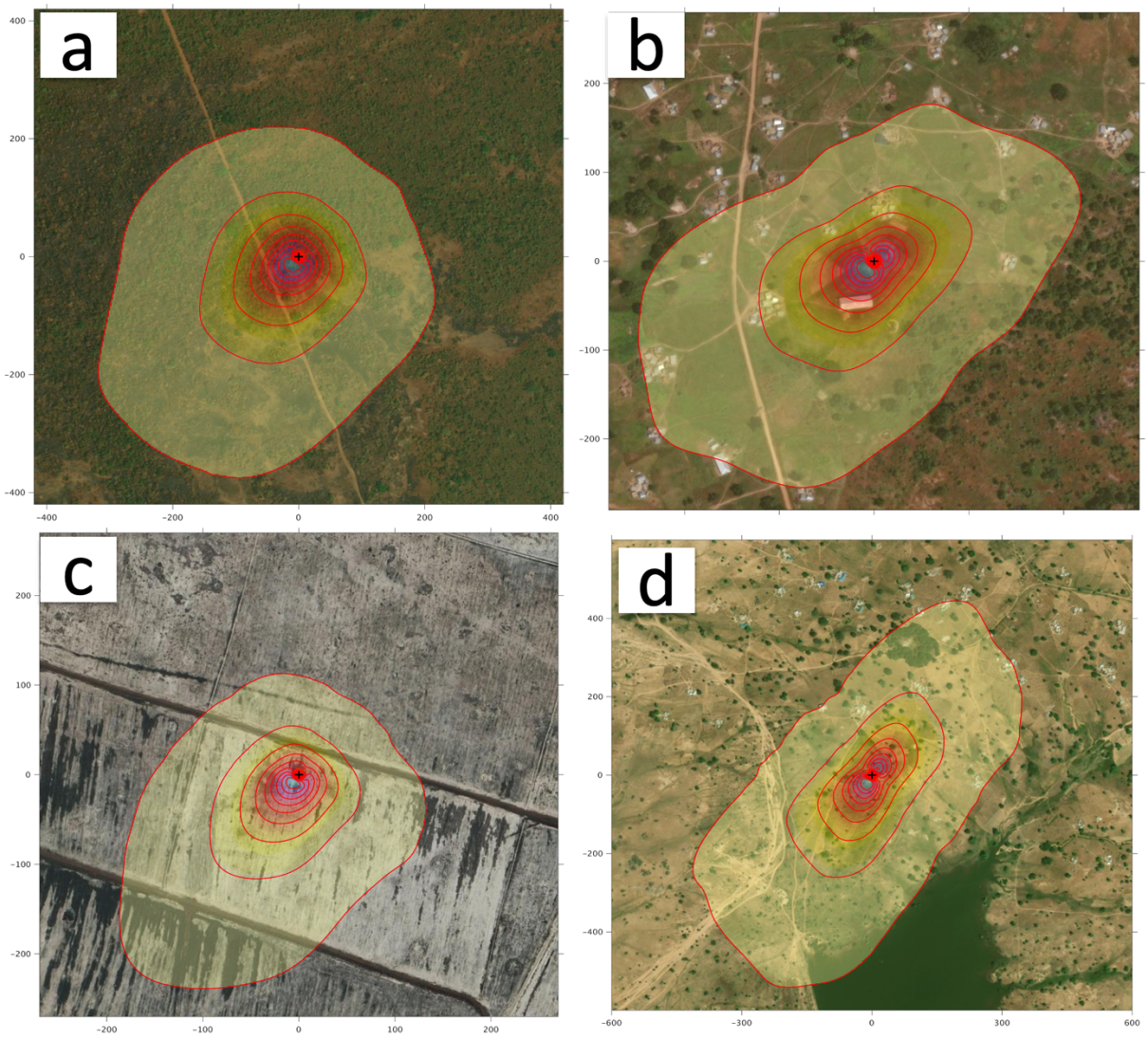

Figure S8: Sample images acquired at different periods from the paddy rice. The canopy camera illustrates the distinct stages of rice cultivation and canopy phenological development for 2023.

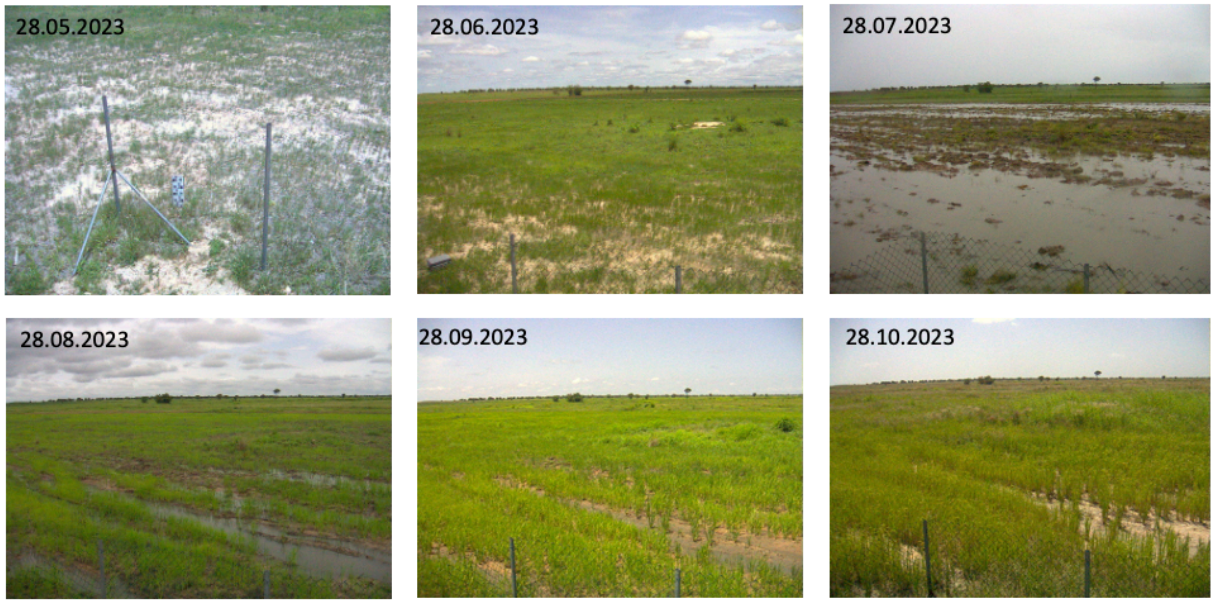

Figure S9: Sample images acquired at different periods of the rainy season from the cropland site. The Camera illustrates the distinct stages of cultivation, canopy phenological development, and land management practices for 2023.

Figure S10: Similar to Figure S9 but for the grassland site.

Figure S11: Similar to Figure S9, but for the savanna reserve forest site over the entire year 2023/2024.